July 30, 2004

LINEAR COLLIDER SIGNALS OF ANOMALY MEDIATED SUPERSYMMETRY BREAKING

Probir Roy

Tata Institute of Fundamental Research

ALCPG meeting, Victoria

- Introduction to AMSB
- Sparticle Spectra of AMSB
- LC Processes and Signals

$$
\begin{aligned}
e^+e^- &\rightarrow \gamma\tilde{\chi}_1^+\tilde{\chi}_1^- \\
e^+e^- &\rightarrow \tilde{e}^+\tilde{e}^-,\ \tilde{\chi}_1^0\tilde{\chi}_2^0,\ \tilde{\chi}_2^0\tilde{\chi}_2^0 \\
e\gamma &\rightarrow \tilde{\nu}\tilde{\chi}_1^- \\
\gamma\gamma &\rightarrow \tilde{\chi}_1^+\tilde{\chi}_1^-\gamma
\end{aligned}
$$

INTRODUCTION TO AMSB

MSSM left-chiral superfields $(\Phi \sim \varphi + \theta\Psi + \theta\theta F)$

$$Q_i = \binom{U_i}{D_i}, L_i = \binom{N_i}{E_i}, H_u = \binom{H_u^+}{H_u^0}, H_d = \binom{H_d^0}{H_d^-} : \ SU(2)_L \text{ doublets, } \tan\beta = \frac{\langle H_u^0 \rangle}{\langle H_d^0 \rangle}.$$

$$\overline{U_i}, \overline{D_i}, \overline{E_i} \qquad\qquad SU(2)_L \text{ singlets}$$

Superpotential

$$\mathcal{W} = h_{ij}^u \ Q_i \cdot H_u U_j + h_{ij}^d \ Q_i \cdot H_d \overline{D_j} + h_{ij}^e \ L_i \cdot H_d \overline{E_j} + \mu H_u \cdot H_d$$

Spontaneous SUSY breaking with just these fields ruled out by Dimopoulos-Georgi sumrule $(m_{\tilde{u}_L}^2 + m_{\tilde{u}_R}^2 - 2m_u^2) + (m_{\tilde{d}_L}^2 + m_{\tilde{d}_R}^2 - 2m_d^2) = 0$

$\therefore$ **SUSY breaking through explicit soft (mass dimension < 4) terms.**

$\longrightarrow$ **MSSM.**

105 new parameters in MSSM.

- squark masses
- slepton masses
- gaugino masses
- A- and B-terms

Effective theory from spontaneous supersymmetry breakdown in a gauge singlet world : HIDDEN SECTOR

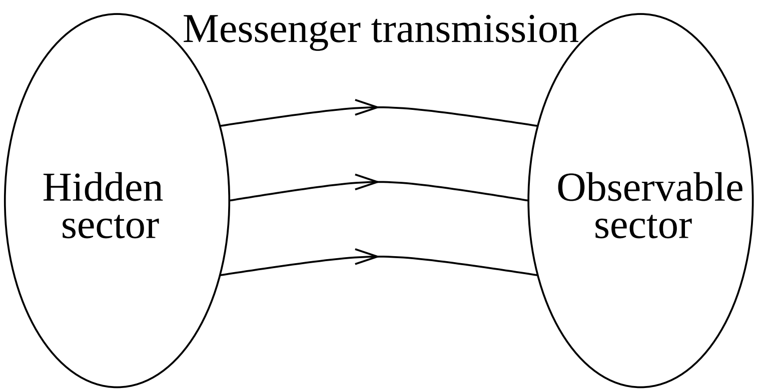

Drastic reduction of parameters in MSSM depending on the mediators: gravity or messenger gauge fields ?

A specially interesting scenario is Anomaly Mediation **AMSB:** a particular case of gravity mediation, with no tree level supergravity couplings between the two sectors. Best realised in higher dimensional theories.

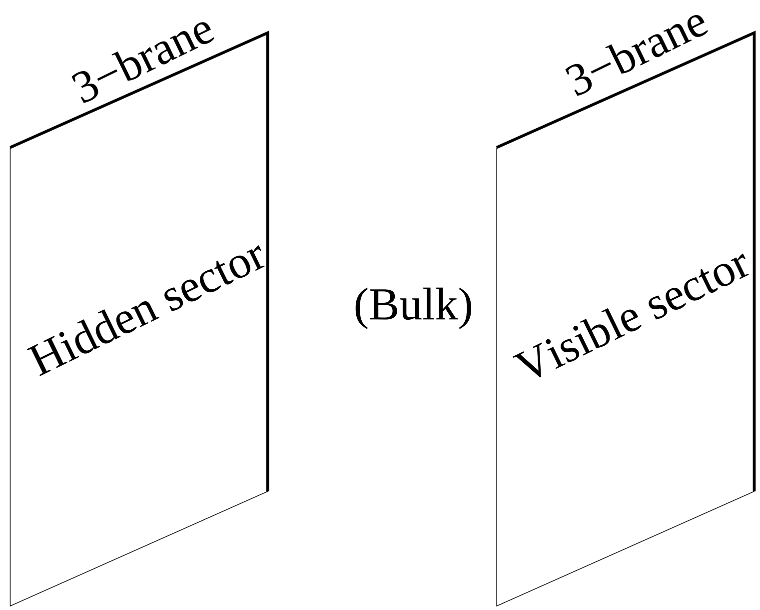

- Tree level supergravity couplings between the two sectors avoided if the branes are well separated by $\sim 10^{16}\ \mathrm{GeV}^{-1}$, say.

- quantum loop-induced superconformal anomaly can cause the transmission of supersymmetry breaking from the hidden to the observable sector.

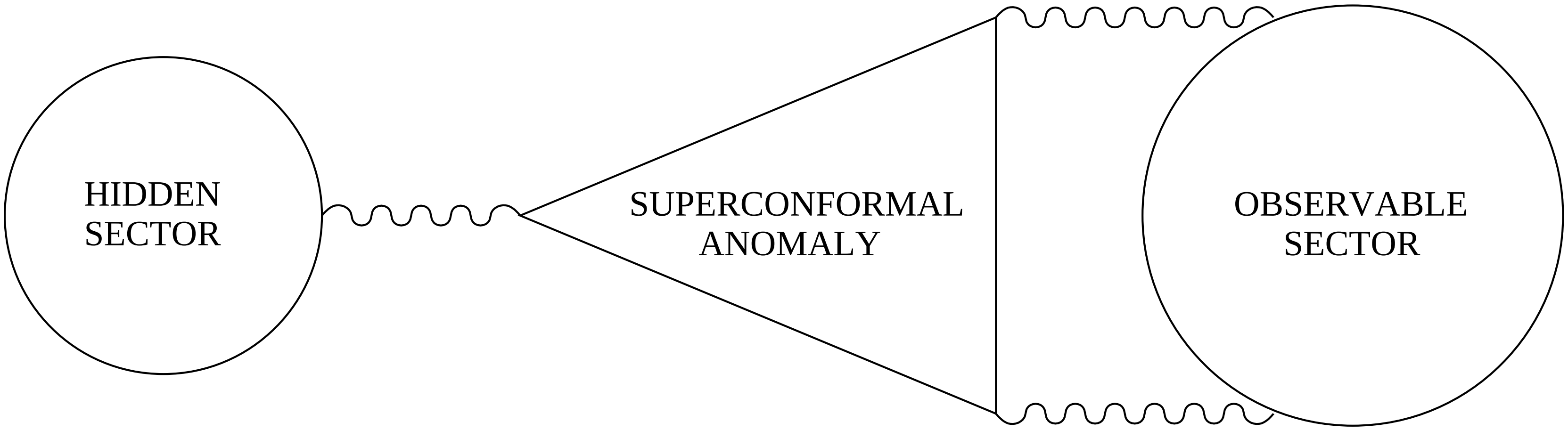

Soft operators $\sim \frac{1}{16\pi^2}\ \frac{<F>}{M_{P\ell}}$ should pertain to EW scale.

Loop factor makes $<F> \gg M_W M_{P\ell}$ and $m_{3/2} \sim 10$ to 100 TeV.

SPARTICLE SPECTRA OF AMSB

Gaugino masses $M_\alpha = \frac{\beta(g_\alpha)}{g_\alpha} M$ $\quad (M_1 : M_2 : M_3)_{EW} \simeq 2.8 : 1 : 7.1$

vs. $\simeq 1 : 2 : 7$

mSUGRA
mGMSB

Sfermion masses $\tilde{m}_i^2 = m_0^2 - \frac{1}{4}\left[\beta(g_\alpha)\frac{\partial\gamma_i}{\partial g_\alpha} + \beta_Y \frac{\partial\gamma_i}{\partial g_Y}\right] m_{3/2}^2$

$m_0^2 =$ **bulk-generated,**
avoids tachyonic sleptons

Randall, Sundrum

Giudice, Wells

Feng, Moroi

Nonminimal versions with extra (exotic) $U(1)$, vector multiplets, gaugino-assisted AMSB . . .

Pomerol, Rattazzi

Kaplan, Kribs

Chacko, Luty, Maksymik, Ponton

Nelson, Weiner

Allanach, Diedes

Two types of mAMSB mass spectra : A and B, including $B1$

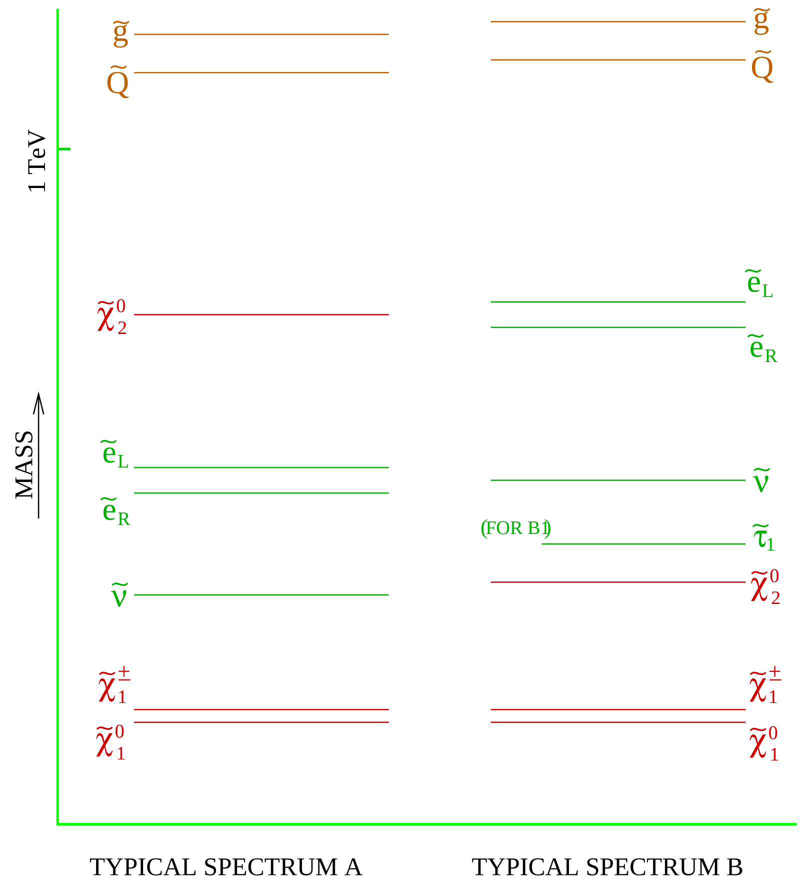

Features of AMSB spectra

- Lightest neutralino/charginos almost winolike : $\tilde{\chi}_1^{\pm} \sim \widetilde{W}^{\pm}, \tilde{\chi}_1^0 \sim \widetilde{W}^0$
- Near mass degeneracy of $\tilde{\chi}_1^0, \tilde{\chi}_1^{\pm}$ (robust)
- Closeness in mass of $\tilde{e}_{L,R}$ (mAMSB)

$\Delta M = M_{\tilde{\chi}_1^\pm} - M_{\tilde{\chi}_1^0}$ small, from $\begin{cases} \text{tree level gaugino-higgsino mixing} \\ \text{one loop contribution} \end{cases}$

165 **MeV** $< \Delta M <$ 800 **MeV.** $\tilde{\chi}_1^\pm$ **quasistable.** Ghosh, P.Roy and S.Roy

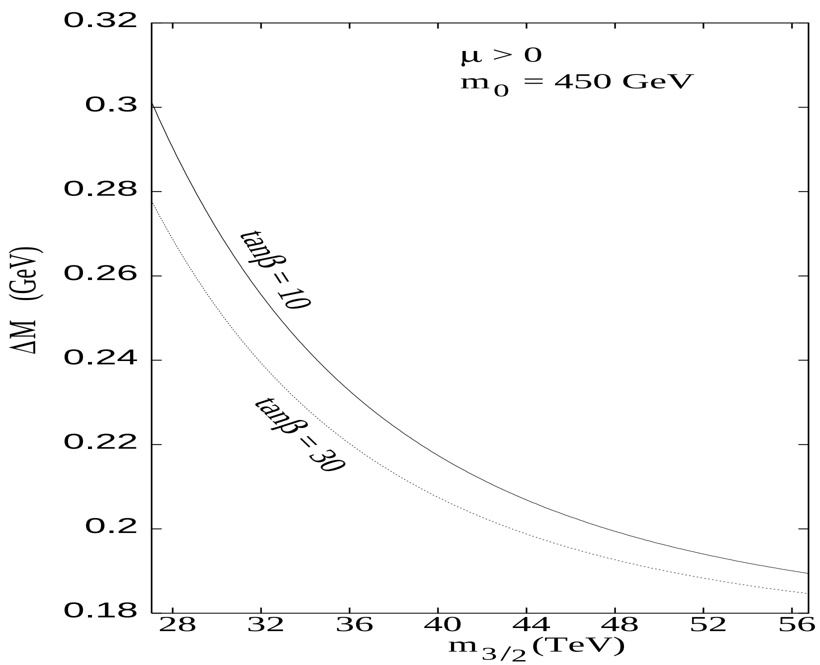

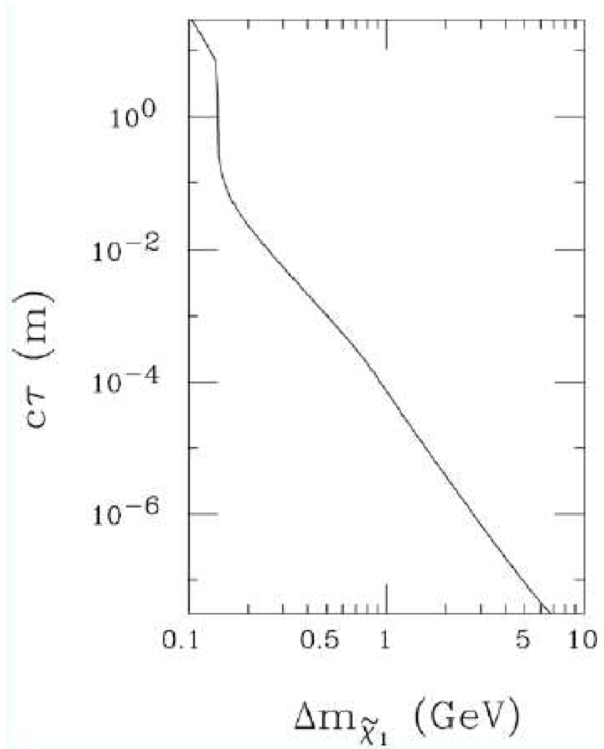

$\tilde{\chi}_1^\pm \to \tilde{\chi}_1^0 + (1, 2)$ **soft pion(s)**

$\tilde{\chi}_1^0 \longrightarrow$ heavy ionizing track X_D, observable vertex displacement?
Characteristic impact parameter distribution of soft pion(s)?

Gunion, Mrenna

Cheng, Dobrescu, Matchev

LEP bounds relevant to AMSB : $m_{\tilde{\chi}_1^\pm} > 86$ GeV. A. Heister et al. ALEPH

$m_{\tilde{\tau}_1} > 82$ GeV. M. Elsing, DELPHI

Additional constraints: $(g-2)_\mu$ and $\Gamma(B_s \to X_s\gamma)$ rule out regions in $m_0, m_{3/2}$ plane, disfavor low $\tan\beta$ AMSB. $\tan\beta >$ 30 fine.

Feng, Moroi

Feng, Matchev

Chattopadhyay, Nath

Baer, Balaz, Fernandis, Tata

Enqvist, Gabrielli, Huitu.

LC PROCESSES AND SIGNALS

Won't discuss hadronic collider signals of **AMSB.** Review Ambrosanio et al. hep-ph/0006162 Mele, hep-ph/0407204

$e^+e^- \to \gamma\tilde{\chi}_1^+\tilde{\chi}_1^-$

Trigger: hard photon $+\not{E}_T + X_D/\pi$ **(**$\pi \equiv$ one or more soft pions**).**

Studied in mSUGRA for $|M_2| \gg |\mu|$ (higgsinolike $\tilde{\chi}_1^0, \tilde{\chi}_1^\pm$**).**

Chen, Drees, Gunion

Detailed analysis in **mAMSB** Datta, Maity

At $\sqrt{s} = 500$ GeV with $\mathcal{L} = 50 fb^{-1}$, with suitably chosen cuts to reduce bkgd, hundreds of events expected for **100 GeV** $< M_{\tilde{\chi}_1^+} < 200$ **GeV.**

- **Track length X_D and impact parameter b of π can be used to enhance S/B.**

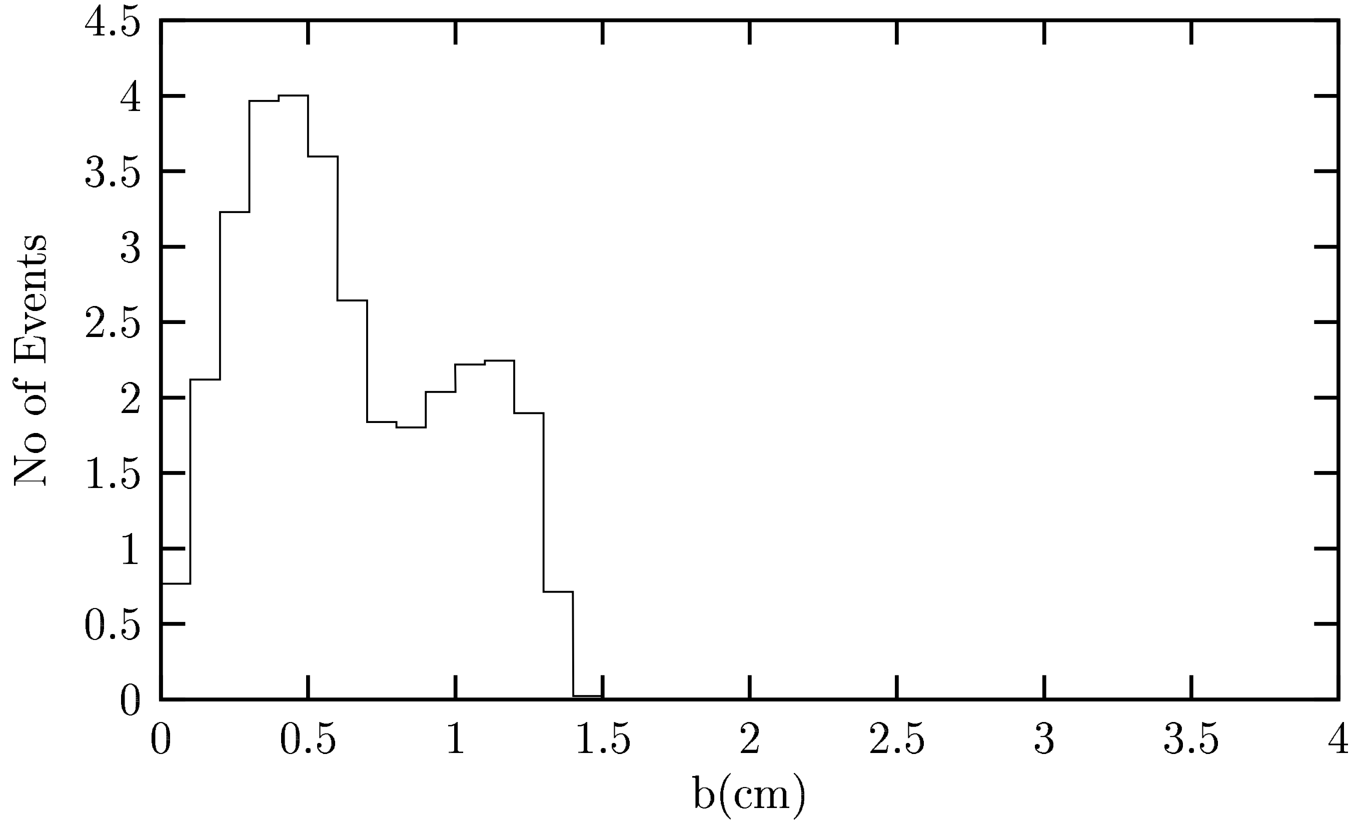

- Determination of $m_{\tilde{\chi}_1^\pm}$ from kinematics and $m_{\tilde{\nu}}$ from production X-section may help distinguish mAMSB from models with $|M_2| \gg |\mu|$ and large $m_{\tilde{\nu}}$.

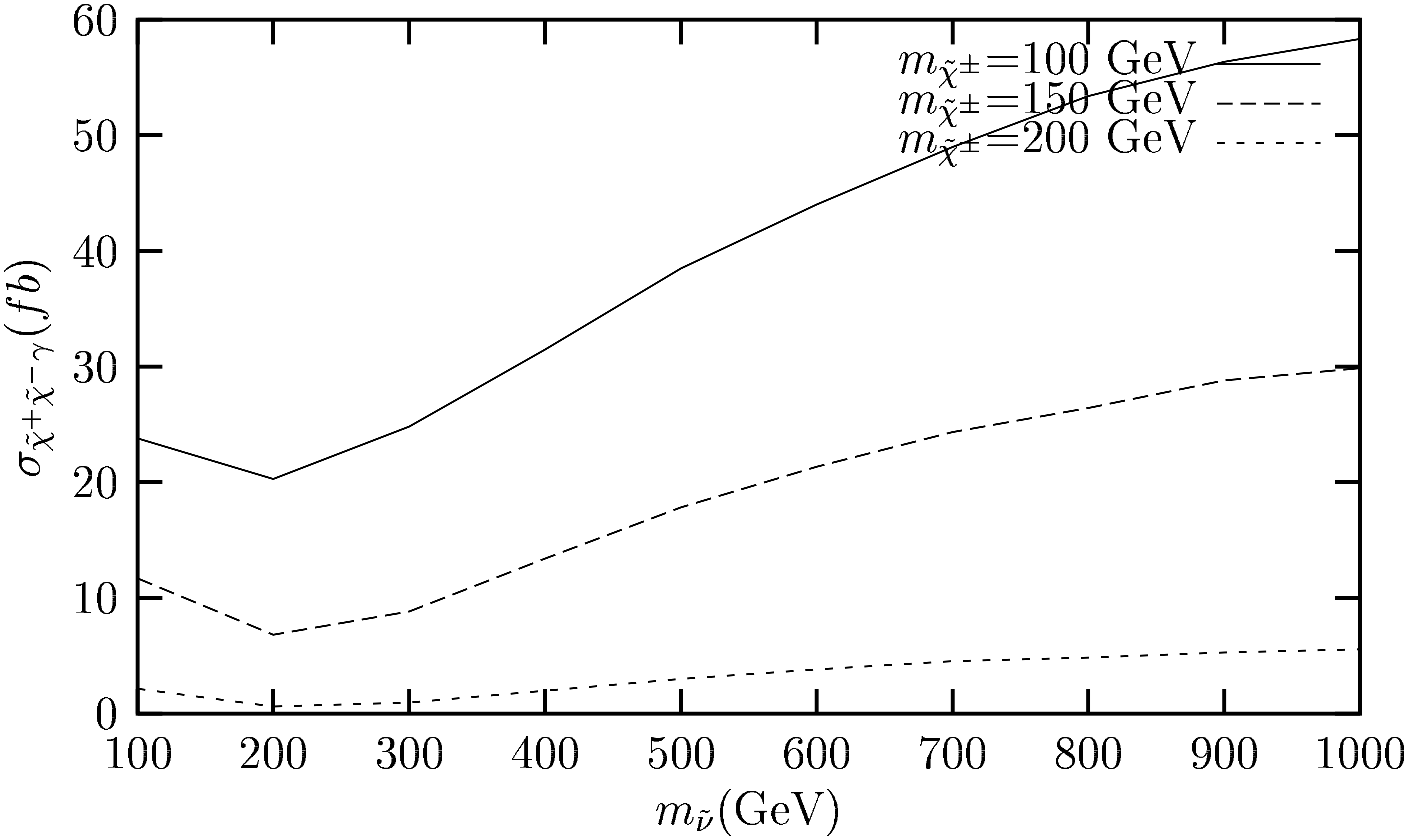

$m_{Z^*} \equiv \frac{1}{2}(P_{e^+} + P_{e^-} - P_r)^{1/2} > m_{\tilde{\chi}_1^\pm}$ for the signal and helps determine $m_{\tilde{\chi}_1^\pm}$.

$e^+e^- \to \tilde{e}_L^\pm\tilde{e}_L^\mp, \tilde{e}_R^\mp\tilde{e}_R^\pm, \tilde{e}_L^\pm\tilde{e}_R^\mp, \tilde{\chi}_1^0\tilde{\chi}_2^0, \tilde{\chi}_2^0\tilde{\chi}_2^0$

Ghosh, Kundu, P.Roy and S.Roy

Decay Patterns $\ell = e, \mu; \pi = X_D$ and/or soft charged pions

	Spectrum A	Spectrum B
Primary decays	$\tilde{\chi}_2^0 \to \tilde{\nu}\bar{\nu}, \bar{\tilde{\nu}}\nu, \tilde{\ell}_L^\pm\ell_L^\mp, \tilde{\ell}_R^\pm\ell_R^\mp$ $\tilde{e}_L \to e\tilde{\chi}_1^0, \nu_e\tilde{\chi}_1^{ch}$ $^{\#}\tilde{e}_R \to e\tilde{\chi}_2^{0*} \to e\bar{\nu}\tilde{\nu}, e\tau\tilde{\tau}_1$ $\tilde{\nu} \to \ell^\mp\tilde{\chi}_1^\pm, \nu\tilde{\chi}_1^0$	$\tilde{e}_L \to e\tilde{\chi}_1^0, e\tilde{\chi}_2^0, \nu_e\tilde{\chi}_1^{ch}$ $^{@}\tilde{e}_R \to e\tilde{\chi}_2^0$ $\tilde{\nu} \to \nu\tilde{\chi}_1^0, \nu\tilde{\chi}_2^0, \ell^\pm\tilde{\chi}_1^\pm$ $\tilde{\chi}_2^0 \to \tilde{\chi}_1^0 h, \tilde{\chi}_1^0 Z, \tilde{\chi}_1^\pm W^\mp$ $\to \tau\tilde{\tau}_1$ (Spectrum B1)
End products	$\tilde{\chi}_2^0 \to \ell^\pm\pi^\mp \not{E}_T, \ell^+\ell^- \not{E}_T, \ell_1^+\ell_2^-\ell_2^\pm\pi^\mp \not{E}_T$ $\tilde{e}_L \to e\not{E}_T, \pi\not{E}_T$ $\tilde{e}_R \to e\not{E}_T, \pi\not{E}_T$ $\tilde{\nu} \to \ell^\pm\pi^\mp \not{E}_T, \not{E}_T$	$\tilde{e}_L \to e\not{E}_T, \pi\not{E}_T, \pi\not{E}_T, e\ell^+\ell^- \not{E}_T, e\ell^\pm\pi^\mp \not{E}_T$ $\tilde{e}_R \to e\not{E}_T, \pi\not{E}_T, e\ell^+\ell^- \not{E}_T, e\ell^\pm\pi^\mp \not{E}_T$ $\tilde{\nu} \to \ell^\pm\pi^\mp \not{E}_T, \ell^+\ell^- \not{E}_T, \not{E}_T$ $\tilde{\chi}_2^0 \to e^\pm\pi^\mp \not{E}_T, \ell^+\ell^- \not{E}_T, {}^\dagger\not{E}_T$ $\to \ell^+\ell^- \not{E}_T, \tau^+\tau^- \not{E}_T$

$^{\#}\tilde{e}_R \not\to e\tilde{\chi}_1^0$, **since $\tilde{\chi}_1^0$ has no bino component.**
$\tilde{e}_R \not\to e\tilde{\ell}_L^\mp\tilde{\ell}_L^\pm$ **since $m_{\tilde{\ell}_L} > m_{\tilde{e}_R}$.**
† **from $\tilde{\chi}_1^0\nu\bar{\nu}$**

$^{@}$**Prompter in Spectrum B than in Spectrum A**

Spectrum	Signals	Parent Channels
A	$e\ \pi$	$\tilde{\nu}\bar{\tilde{\nu}}$, $\tilde{e}_L^+\tilde{e}_L^-$, $\tilde{e}_L^\pm\tilde{e}_R^\mp$, $\tilde{\chi}_1^0\tilde{\chi}_2^0$, $\tilde{\chi}_2^0\tilde{\chi}_2^0$
	$\mu\ \pi$	$\tilde{\nu}\bar{\tilde{\nu}}$, $\tilde{\chi}_1^0\tilde{\chi}_2^0$, $\tilde{\chi}_2^0\tilde{\chi}_2^0$
	$e^+\ e^-\ \ell\ \pi$	$\tilde{e}_R^+\tilde{e}_R^-$, $\tilde{e}_L^\pm\tilde{e}_R^\mp$, $\tilde{\chi}_1^0\tilde{\chi}_2^0$, $\tilde{\chi}_2^0\tilde{\chi}_2^0$
	$\mu^+\ \mu^-\ \ell\ \pi$	$\tilde{\chi}_1^0\tilde{\chi}_2^0$, $\tilde{\chi}_2^0\tilde{\chi}_2^0$
	$\ell_1\ \ell_1\ \ell_2\ \ell_2\ \ell_3\ \pi$	$\tilde{\chi}_2^0\tilde{\chi}_2^0$ $(\ell_{1,2,3} = e, \mu)$
B	$e\ \pi$	$\tilde{\nu}\bar{\tilde{\nu}}$, $\tilde{e}_L^+\tilde{e}_L^-$, $\tilde{e}_L^\pm\tilde{e}_R^\mp$, $\tilde{\chi}_1^0\tilde{\chi}_2^0$, $\tilde{\chi}_2^0\tilde{\chi}_2^0$
	$\mu\ \pi$	$\tilde{\nu}\bar{\tilde{\nu}}$, $\tilde{e}_L^+\tilde{e}_L^-$, $\tilde{\chi}_1^0\tilde{\chi}_2^0$, $\tilde{\chi}_2^0\tilde{\chi}_2^0$
	$e\ \ell_1^\pm\ \ell_2^\mp\ \pi$	$\tilde{e}_R^+\tilde{e}_R^-$, $\tilde{e}_L^\pm\tilde{e}_R^\mp$, $\tilde{e}_L^+\tilde{e}_L^-$, $\tilde{\nu}\bar{\tilde{\nu}}$, $\tilde{\chi}_2^0\tilde{\chi}_2^0$ $(\ell_{1,2} = e, \mu)$
	$\mu\ \mu^+\ \mu^-\ \pi$	$\tilde{\chi}_2^0\tilde{\chi}_2^0$, $\tilde{\nu}\bar{\tilde{\nu}}$
	$e^+\ e^-\ \ell_1^+\ \ell_1^-\ \ell_2\ \pi$	$\tilde{e}_L^+\tilde{e}_L^-$, $\tilde{e}_R^+\tilde{e}_R^-$, $\tilde{e}_L^\pm\tilde{e}_R^\mp$ $(\ell_{1,2} = e, \mu)$

- Same signals possible in Specta **A** and **B**, though parent sources may be different.
- $3\ell\pi$, i.e. trilepton $+X_D$ and/or soft pion(s) especially interesting. For Spectrum B (not for Spectrum A), $\ell^+\ell^-$ must have mass peak at M_Z. Discriminant between the two spectra.

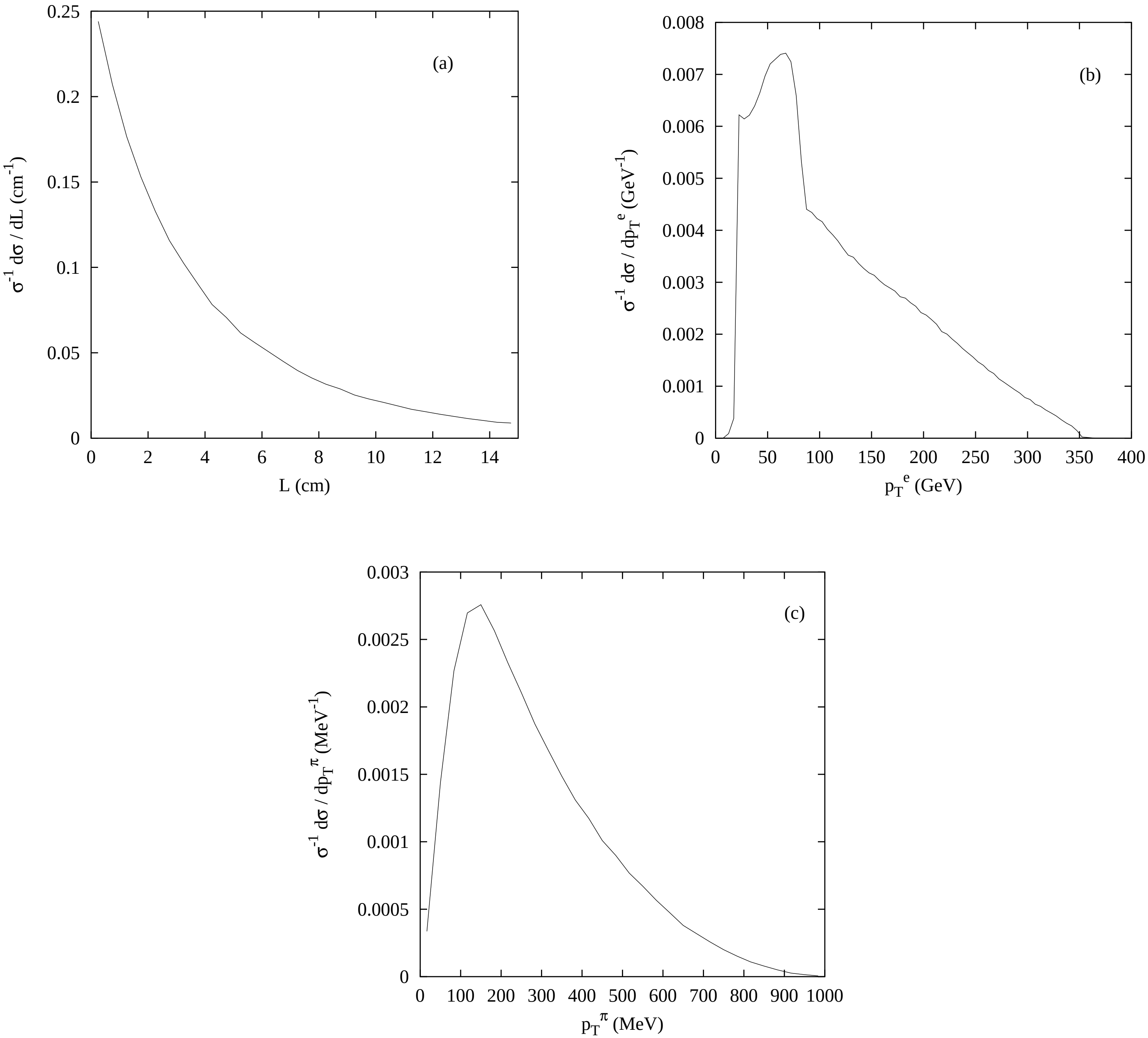

Detailed study of Spectrum A

Spectrum A

Signal	PS	Cross Sections (fb)						
		$\tilde{\nu}\bar{\tilde{\nu}}$	$\tilde{e}_L\bar{\tilde{e}}_L$	$\tilde{e}_R\bar{\tilde{e}}_R$	$\tilde{e}_L\bar{\tilde{e}}_R + \tilde{e}_R\bar{\tilde{e}}_L$	$\tilde{\chi}_1^0\tilde{\chi}_2^0$	$\tilde{\chi}_2^0\tilde{\chi}_2^0$	Total
$e\pi + \not{E}_T$	a	40.27	46.7	-	0.00029	2.46	0.118	89.54
	b	40.94	45.09	-	0.000121	2.48	0.14	88.65
	c	43.03	44.44	-	2.55×10^{-5}	2.14	0.13	89.74
	d	30.17	31.63	-	3.24×10^{-8}	1.74	0.032	63.57
	e	26.4	24.33	-	0.0	1.35	0.011	52.09
	f	17.28	13.43	-	0.0	0.99	0.003	31.70
$ee\mu\pi + \not{E}_T$	a	-	-	1.36×10^{-4}	0.010	1.44	0.159	1.61
	b	-	-	3.65×10^{-4}	0.012	1.32	0.174	1.50
	c	-	-	0.00	0.018	1.19	0.116	1.32
	d	-	-	0.00	2.3×10^{-5}	0.014	0.033	0.047
	e	-	-	0.00	4.15×10^{-5}	0.011	0.008	0.019
	f	-	-	0.00	2.02×10^{-5}	0.006	0.001	0.007
$ee\pi\pi + \not{E}_T$	a	24.21	-	-	0.014	-	0.0511	24.27
	b	24.94	-	-	0.016	-	0.0648	25.02
	c	27.66	-	-	0.026	-	0.0604	27.74
	d	16.45	-	-	2.7×10^{-5}	-	0.0119	16.46
	e	14.62	-	-	5.04×10^{-5}	-	0.0044	14.62
	f	8.66	-	-	2.41×10^{-5}	-	0.000972	8.66

$e\gamma$ Collision

$e^-\gamma \to \tilde{\nu}\tilde{\chi}_1^-, \quad \tilde{\nu} \to e^-\tilde{\chi}_1^+ \to e^-\pi^+\tilde{\chi}_1^0, \quad \tilde{\chi}_1^- \to \pi^-\tilde{\chi}_1^0$ Choudhury, Ghosh, Roy

Observable final configuration $e\pi^-\pi^+\not{E}_T$

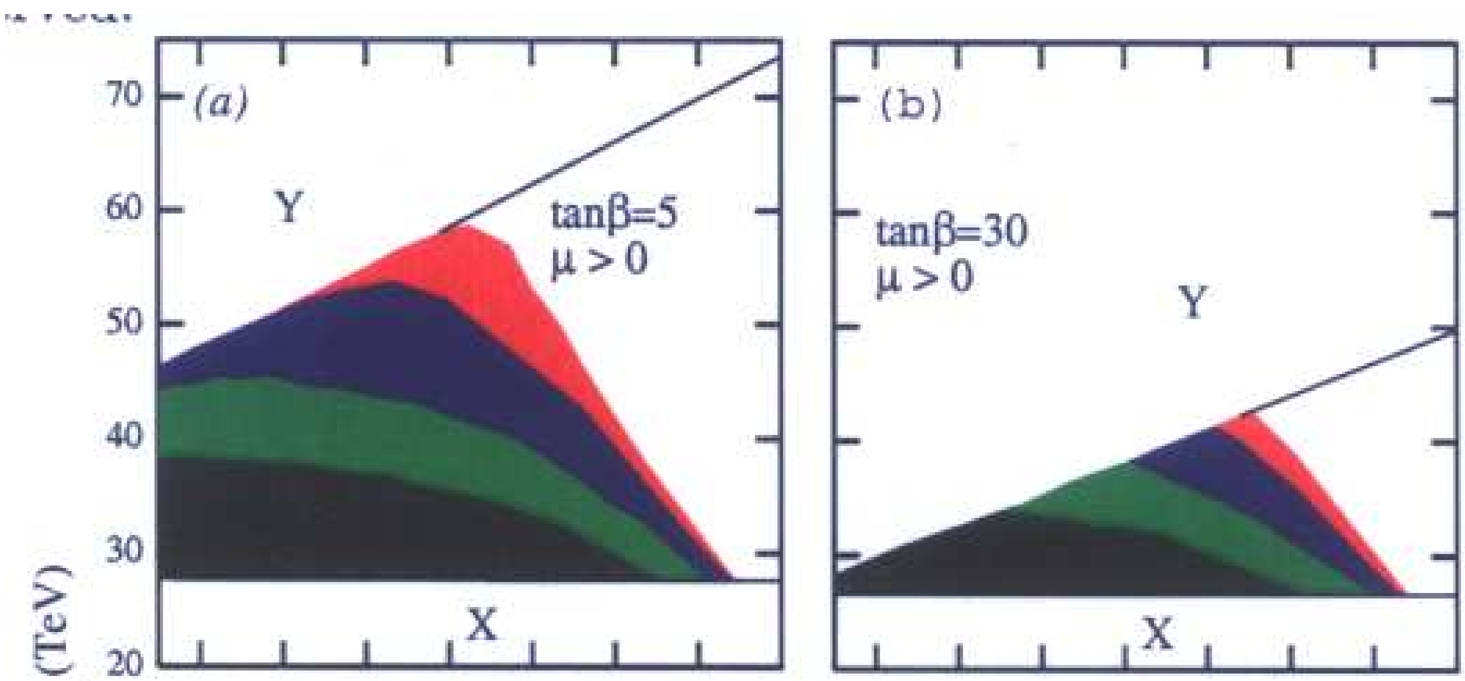

$m_{3/2}$ vs.$\mathrm{m_0}$ plot, 20 TeV $< \mathrm{m}_{3/2} <$ 70 TeV, 0.25 TeV $< \mathrm{m_0} <$ 0.4 TeV, $\mathrm{P_e} = -0.8$, $\mathrm{P_L} = +1$.

X ruled out by LEP limit on chargino mass, Y by the requirement of $\tilde{\chi}_1^0$ being the LSP. The top three shaded regions correspond to X-section in the ranges (0.1–5) fb, (5–50) fb and (50–150) fb while the lowermost region to (150–470) fb in (a) and (150–390) fb in (b).

Can determine $m_{\tilde{\nu}}, m_{\tilde{\chi}_1^\pm}$ from electron energy spectrum endpoints.

$$\frac{m_{\tilde{\nu}}^2 - m_{\tilde{\chi}_1^\pm}^2}{2(E_{\tilde{\nu}}^{\max} + k_{\tilde{\nu}}^{\max})} \leq E^e \leq \frac{m_{\tilde{\nu}}^2 - m_{\tilde{\chi}_1^\pm}^2}{2(E_{\tilde{\nu}}^{\max} - k_{\tilde{\nu}}^{\max})},$$

$$E_{\tilde{\nu}}^{\max} = \frac{1}{4 y_{\max}\sqrt{s}}\left[(1+y_{\max})(y_{\max}s + m_{\tilde{\nu}}^2 - m_{\tilde{\chi}_1^\pm}^2) + (1-y_{\max})\sqrt{(y_{\max}s + m_{\tilde{\nu}}^2 - m_{\tilde{\chi}_1^+}^2)^2 - 4 y_{\max} s m_{\tilde{\nu}}^2}\right]$$

$$k_{\tilde{\nu}}^{\max} = \sqrt{E_{\nu}^{\max 2} - m_{\tilde{\nu}}^2}$$

and $y_{\max}$ = maximum value of the fraction of $e^\pm$ energy carried off by the reflected photon beam

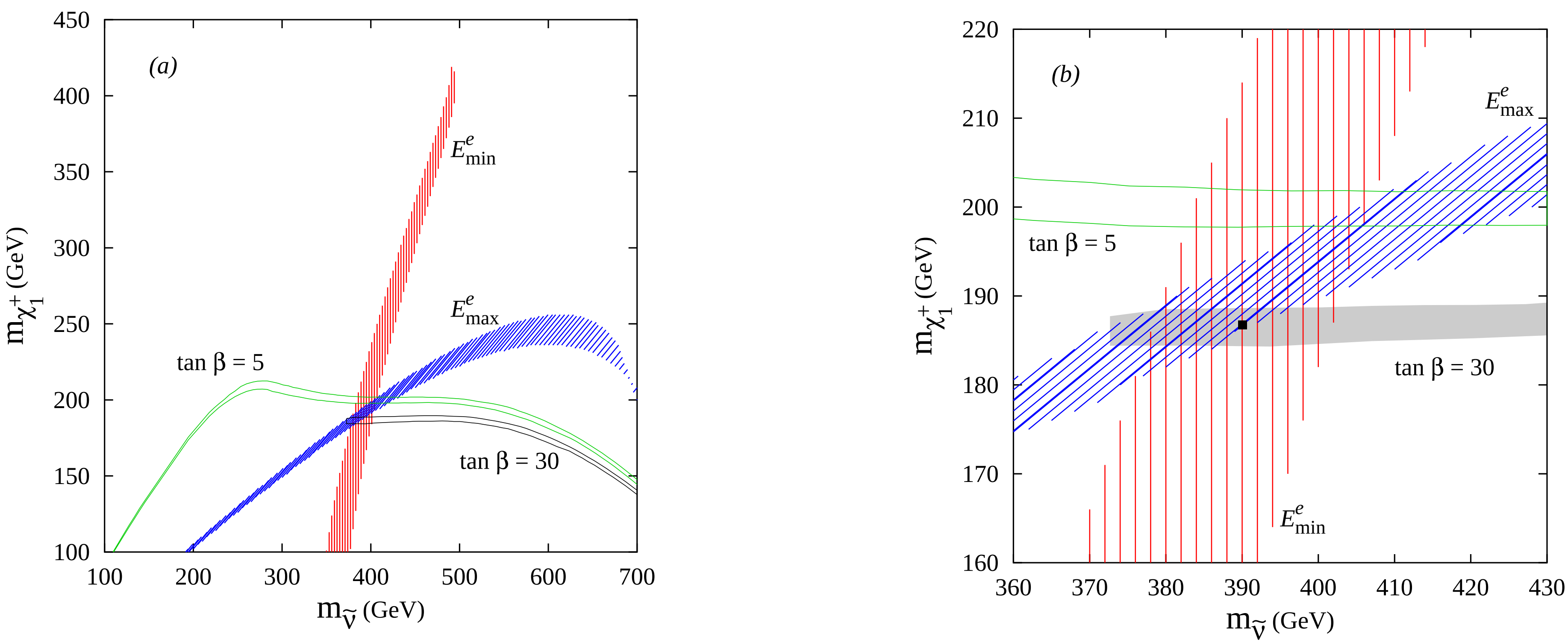

Sensitive upto $m_{\tilde{\chi}_1^\pm} \sim 200$ GeV and $m_{\tilde{\nu}}$ upto 400 GeV for $\sqrt{s} = 500$ GeV and $\int dt\mathcal{L} = 50\ \mathrm{fb}^{-1}$.

$\gamma\gamma$ collision

$\gamma\gamma \to \tilde{\chi}_1^+ \tilde{\chi}_1^- \gamma,\ \tilde{\chi}_1^\pm \to \tilde{\chi}_1^0 \pi^\pm$ Choudhury, Mukhopadhyaya, Rakshit, Datta

Chargino mass measurable from this process.

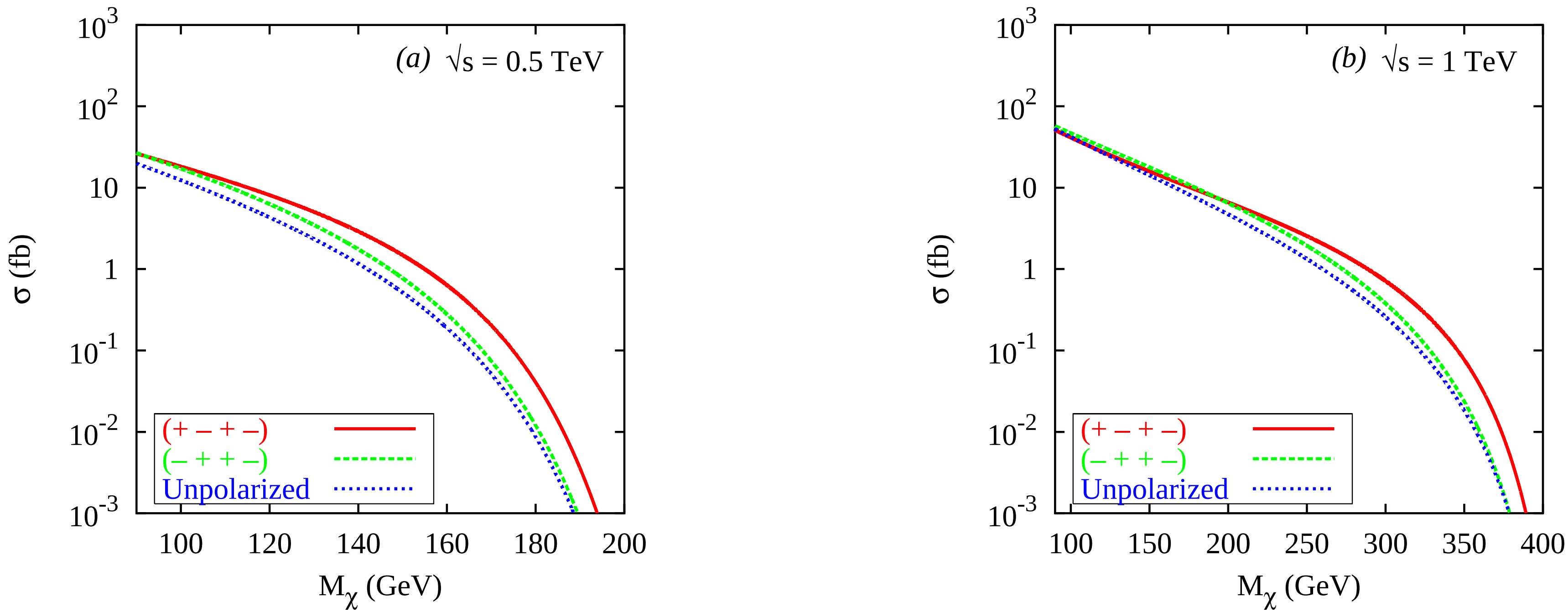

Signal cross section vs. e^+e^- CM energy, with $p_T^\gamma > 10$ GeV.

$\int dt\mathcal{L} = 100\ \text{fb}^{-1}$ at $\sqrt{s} = 500$ GeV sensitive upto $m_{\tilde{\chi}_1^\pm} \sim 165$–$170$ GeV. Mass reach roughly doubled at $\sqrt{s} = 1$ TeV.

Acknowledgement

I have benefitted enormously from discussions with my collaborators Dilip Ghosh, Anirban Kundu and Sourov Roy.